

We are IntechOpen, the world's leading publisher of Open Access books Built by scientists, for scientists

4,800

Open access books available

122,000

International authors and editors

135M

Downloads

Our authors are among the

154

Countries delivered to

TOP 1%

most cited scientists

12.2%

Contributors from top 500 universities



WEB OF SCIENCE™

Selection of our books indexed in the Book Citation Index
in Web of Science™ Core Collection (BKCI)

Interested in publishing with us?
Contact book.department@intechopen.com

Numbers displayed above are based on latest data collected.
For more information visit www.intechopen.com



RF Energy Harvesting System and Circuits for Charging of Wireless Devices Using Spectrum Sensing

Naser Ahmadi Moghaddam and Alireza Maleki

Abstract

Recently, lots of works have been done on the optimal power management of wireless devices. This leads to the main idea of ambient energy harvesting. Among various energy harvesting approaches, one is to use radio waves existing in the ambient environment for battery charging, called RF energy harvesting. In this chapter, in order to improve the RF energy harvesting performance, we utilize spectrum sensing to allow the wireless devices to select the frequency band with maximum power that exceeds a predefined threshold to charge the device (this power threshold can be determined according to battery type and its required charging power) and the device can use this power for battery charging. Also, a novel voltage multiplier circuit is proposed. By means of simulations and experimental tests, it can be seen that after detection of our desired 1 mW RF signal, system output power is about $532\mu\text{ W}$ and $450\mu\text{ W}$ in simulation and practical situations respectively.

Keywords: energy harvesting, voltage multiplier, OFDM, spectrum sensing

1. Introduction

Recently, with the rapid growth of wireless communication systems, researchers have studied various challenges about improvement of these systems from many aspects such as performance, error optimization, hardware design and implementation and etc. with introducing the wireless sensor networks, Internet of Things (IoT) and robotics, one of the main challenges appeared is the energy consumption of these systems and how to provide reliable and low cost power supply to feed these systems as long as possible with high durability. That is the main reason for all of the researches conducted on energy harvesting. Various methods and approaches are presented to tackle the issue e.g. improvement of batteries structure and their capacity, piezoelectric materials and movement of human body part to produce the required power mostly for wearable devices, or thermal and magnetic energy harvesting approaches.

Mainly, there are two energy sources: mechanical and magnetic waves [1]. For energy harvesting purposes, as in [2–5], natural sources like solar energy wind, vibrations and movement of human body parts or magnetic waves can be exploited. Here in this chapter, our focus is on a specific kind of electromagnetic source, Radio Frequency (RF) signal, which is produced by the oscillation of photons in a certain frequency and used for transmitting data and information in communication systems.

Examples of these transceivers in today's world are Frequency Modulation (FM) radio, Analog TV (ATV), Digital TV (DTV), mobile and cellular networks and Wi-Fi. To have a more clear understanding of the issue and seeing RF signals as a energy source, in **Figure 1**, DTV and cellular signal spectrums for Tokyo City and Yokohama City are indicated [6]. As it can be seen in this figure, for some certain frequencies, the measured power is about 0 and -20 dB.

By saying RF energy harvesting, we mean that we capture the energy from the RF signal existing in the ambient and transform this power into DC power and using it for supplying battery. Passive ambient RF energy harvesting is exactly defined as this procedure [7]. In this case, sources can be FM radio, Wi-Fi, DTV or military communication transmitters [8] and the amount of energy harvested from these sources is in the order of 1 to $10 \frac{\mu W}{cm^2}$ [9]. Also there is another type of RF energy harvesting, i.e. RF energy harvesting from a dedicated source. In this scenario, the amount of harvested energy is higher comparing to passive ambient case and is in the order of $50 \frac{\mu W}{cm^2}$ [9]. One example for this category is RFID chips [10].

1.1 Preprocessing in energy harvesting system

Spectrum is a scarce source. In wireless communication systems, efforts have been made to use frequency spectrum with policies and priorities in order to maximize the spectrum efficiency. The main idea here is to allocate empty spectrum holes over time, frequency and space to secondary users while the interference with primary user is minimum. Several approaches are proposed for spectrum sensing, such as energy detection [11–13], matched filter [11, 12, 14], cyclostationary detection [15, 16], spectrum sensing based on covariance matrix [17, 18] and wavelet based spectrum sensing [19]. By studying energy detection, it can be understood that this approach is based on detecting the signal power such a way that secondary users detect the signal power received from primary users. Then they compare it to some predefined threshold level and then decide whether they can use the primary frequency band or not. Well, here is the novel preprocessing idea which we are exploited in this chapter:

“In RF energy harvesting, we use RF signal power and convert it to DC power for charging batteries. On the other hand, energy detection algorithms give us the

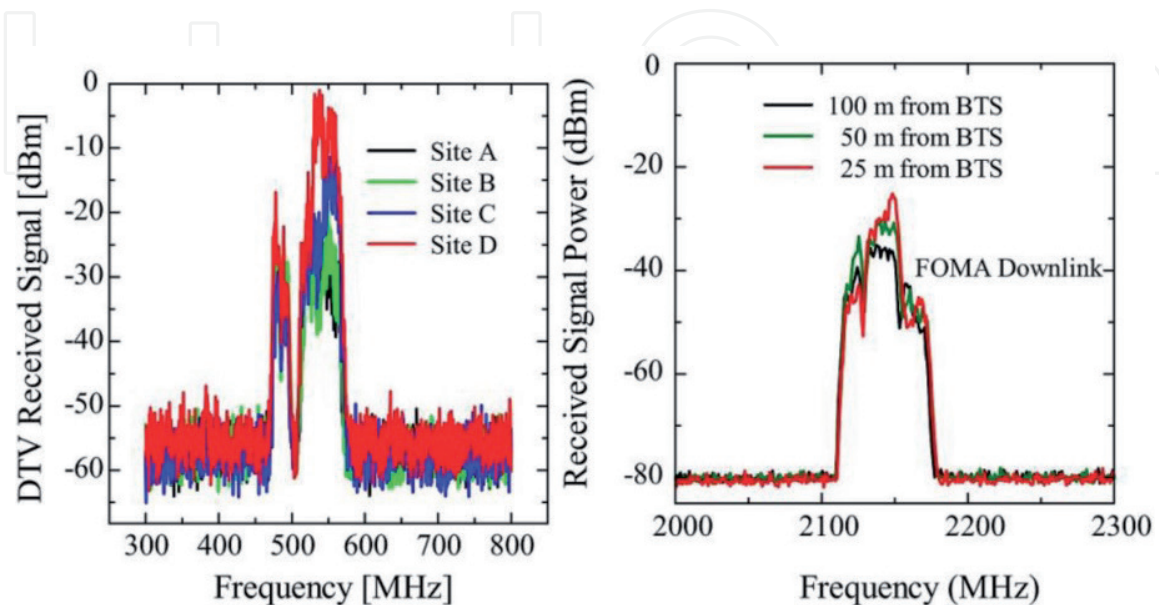


Figure 1. DTV signal spectrum measured in Tokyo City (left side graph) and Cellular signal spectrum measured in Yokohama City (right side graph) [6].

ability to detect the ambient signal power and compare it to a predefined threshold level. So, we do the same here as well. But with the goal of detecting a strong RF signal. In other words, by exploiting this preprocessing, we compare our received RF signal power and if it is greater than a threshold, then we will decide that frequency contains our required power for energy harvesting purposes and switch our circuit to that frequency. In the simulation process, this threshold is set to 0 dBm which is a reasonable and practical assumption based on **Figure 1**.”

2. Proposed method

Our proposed system is indicated in **Figure 2**. As it is indicated in this figure, by preprocessing stage, the frequency containing the high amount of energy is selected. After that, this signal is selected as the input of matching circuit and rectified. Then a DC-DC converter circuit is used to level up the DC signal and finally it is fed to the battery for charging.

2.1 Battery model

For simulation stage and performance evaluation of our proposed system, we must be able to model the battery that we intend to charge. There are various battery models with different structures and complexities. Electrochemical models [20–22] are usually used for battery physical design, performance and power generation optimization. Mathematical models [23–26], are much more effective. Random events for predicting battery systematic behaviors like battery life time and efficiency are discussed using mathematical equations. Electrical models [27–33] are placed somewhere between mathematical and chemical models in terms of accuracy and utilize the combination of voltage sources, resistors and capacitors.



Figure 2.
Schematic of proposed system.

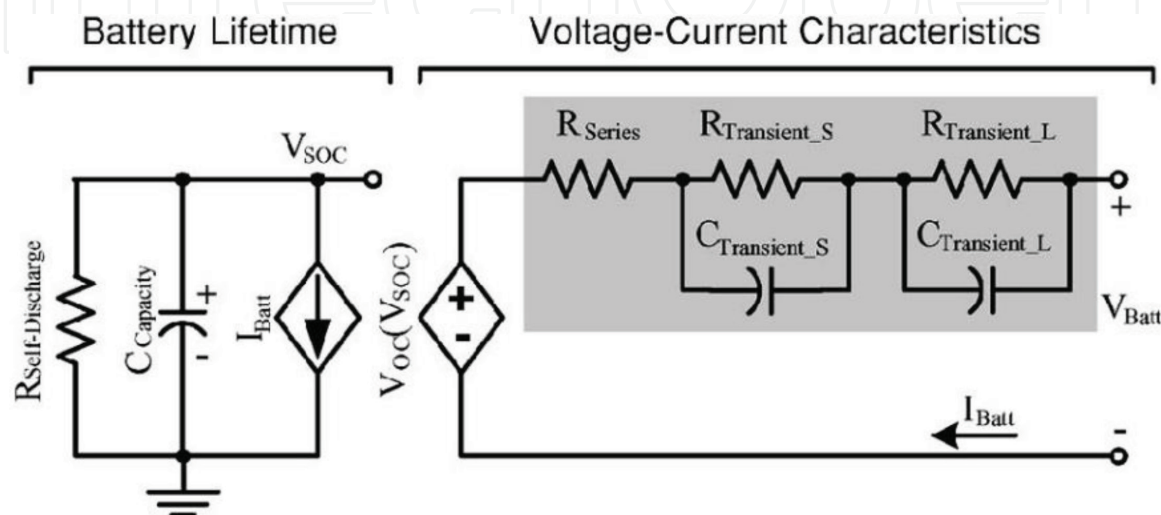


Figure 3.
Battery model [34].

For the goal of this chapter, an accurate and effective battery model is proposed based on battery model proposed in [34]. This model provides an easy extraction procedure, gives run time, static and transient responses and also contains all of the electrodynamic characteristics of the batteries. **Figure 3** shows this proposed model.

3. Results

Simulation results and fabrication of our system is presented in this section. Spectrum sensing, circuits and antenna are simulated using MATLAB, Advance Design System (ADS) and Computer Simulation Technology (CST) software respectively. We consider the frequency band 500 MHz to 1 GHz for maximum power RF signal extraction. At the end, our fabricated charger circuit is tested in laboratory environment.

3.1 Spectrum sensing simulations

We consider M random base stations in the aforementioned frequency band. Using OFDM transmitter, the output signal is generated and by exploiting energy detection, our desired RF signal for energy harvesting circuit is obtained. Parameters of simulation are given in **Table 1**. Note that for digital to analog converter, a 13th order Butterworth filter is used (normalized cut off frequency equals to $\frac{1}{20}$).

RC pulse shaping time response is as follows [35].

$$S_{RC}(t) = \text{sinc}\left(\frac{t}{T_s}\right) \times \frac{\cos\left(\frac{\pi\alpha t}{T_s}\right)}{1 - \frac{4\alpha^2 t^2}{T_s^2}} \quad (1)$$

where α and T_s are roll-off factor (takes values from 0 to 1) and symbol repetition rate respectively.

As it can be seen in **Figure 4**, there are four signals available in the spectrum and in order to find the RF signal with maximum power, the area under each signal should be calculated i.e. its power. After applying energy detection we find that in this case, maximum power RF signal happened at 915 MHz. Therefore, the filter is set to select this signal out of the spectrum.

Parameters	Value (OFDM)
Number of sub-carriers	2048
Occupied of sub-carriers	1024
Sampling frequency (MHz)	20
Number of oversampling	4
Pulse shaper	Raised cosine
Number of random frequency	4
IFFT length	4096
Bandwidth (MHz)	10

Table 1.
Stimulation parameters.

After finding the frequency in which our desired RF signal exists, spectrum should be fed to a filter with the central frequency of 915 MHz and the bandwidth of 10 MHz. In **Figure 5**, filter characteristics in terms of frequency response is given. Note that this filter has the ability to be tuned to select the maximum frequency each time. Also, this filter should reject the rest of frequency band otherwise we face some challenges such as power loss and circuit design complexity.

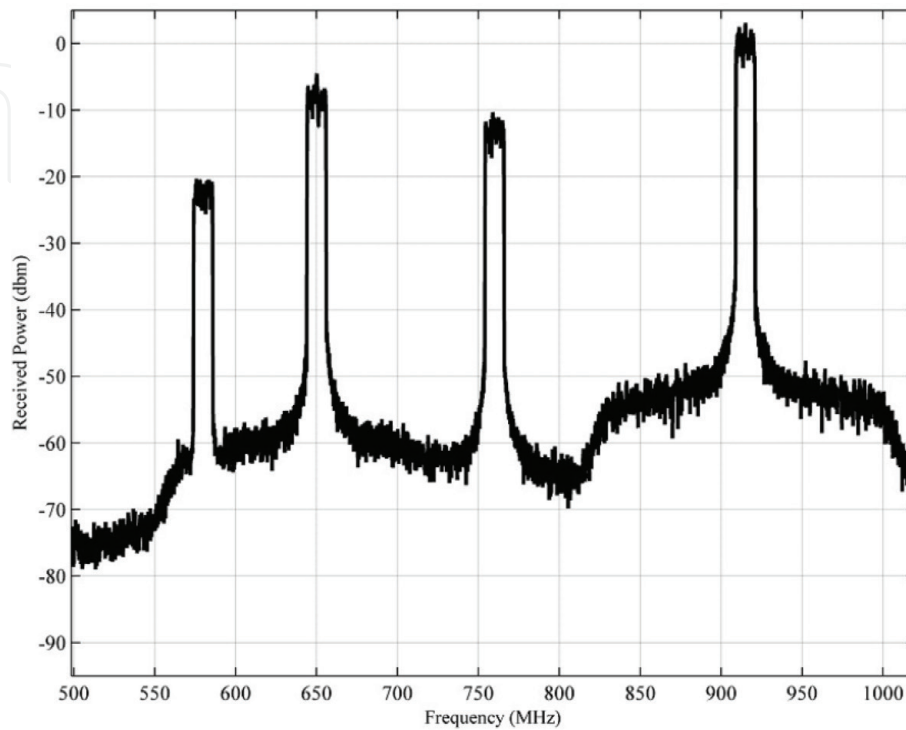


Figure 4.
Frequency response of OFDM transmitter in our frequency band with QPSK modulation in receiver end.

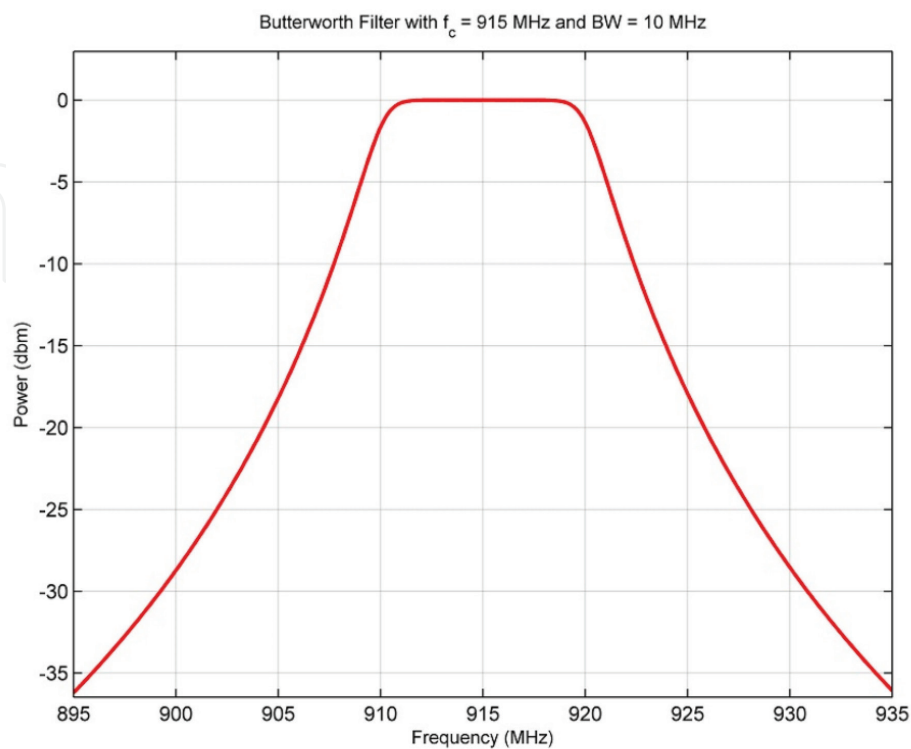


Figure 5.
Frequency response of Butterworth filter with central frequency of 915 MHz and bandwidth of 10 MHz.

Figure 6 shows power for filter, spectrum and the output of filter (Antenna input signal). We use OFDM transmitter as mentioned earlier with QPSK modulation.

3.2 Circuit design and simulation

In previous section, RF signal with maximum power is identified and extracted from spectrum. Now, this signal represents the input of our charging circuit. We assume a 1 mW signal with the frequency of 915 MHz as our input to execute our

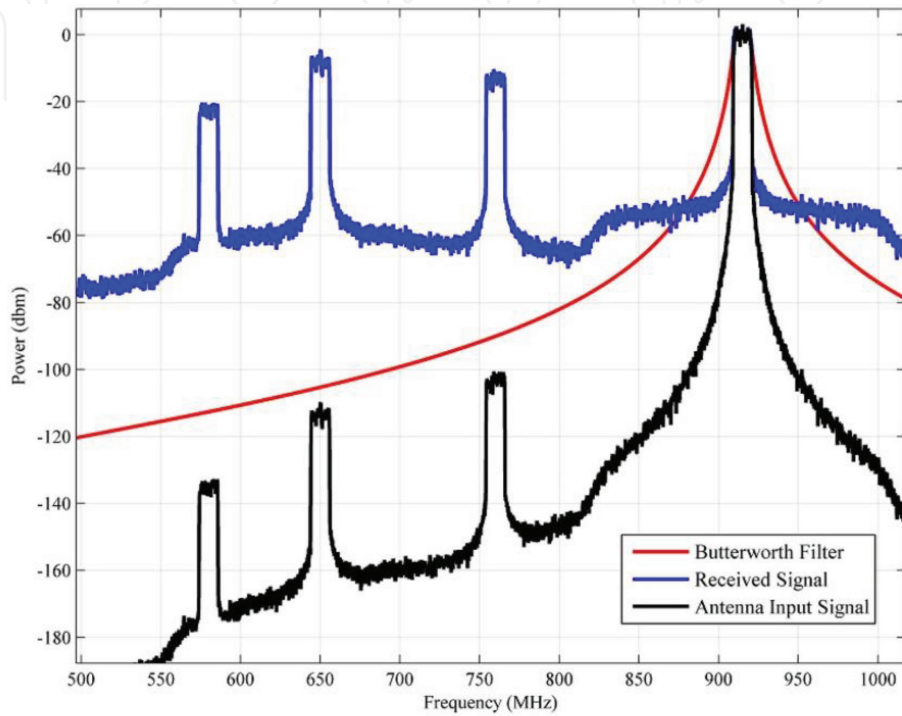


Figure 6.
Frequency response of power spectrum, filter and filter output for OFDM transmitter with QPSK modulation.

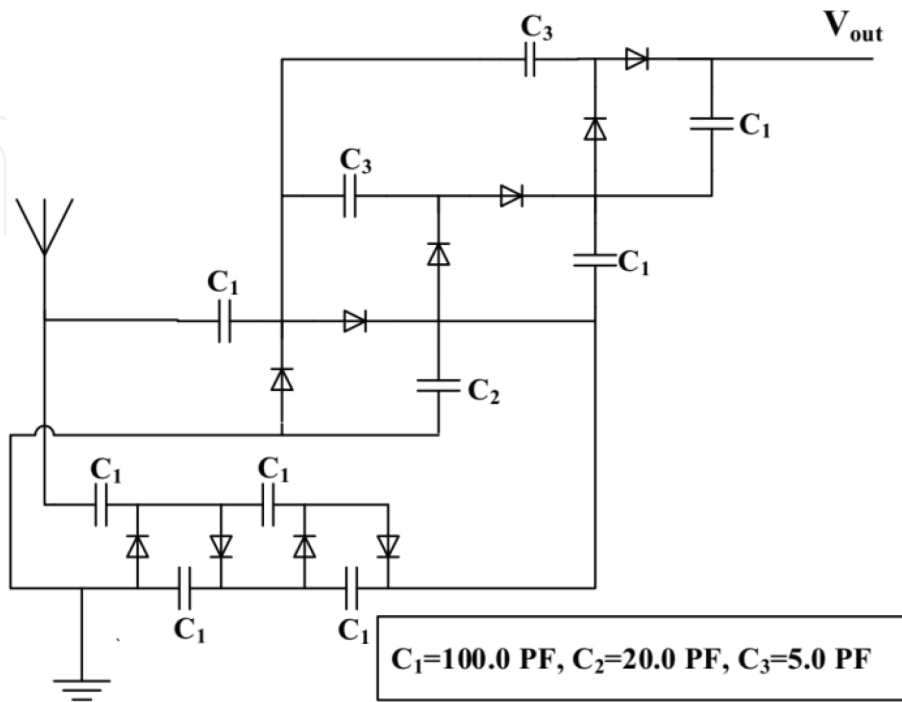


Figure 7.
Proposed voltage multiplier circuit.

simulation in ADS. First, we need to increase the DC level of our signal using a DC voltage multiplier circuit as it is shown in **Figure 7**. Note that we have a 4-stage and a 6-stage voltage multiplier in our proposed circuit. The connection between these two multipliers results in increasing of the output voltage.

In **Figure 8**, Efficiency of the rectifier circuit is shown versus different values of P_{in} . As it can be seen, when the input power is 0 dbm, highest efficiency is obtained at the frequency of 915 MHz.

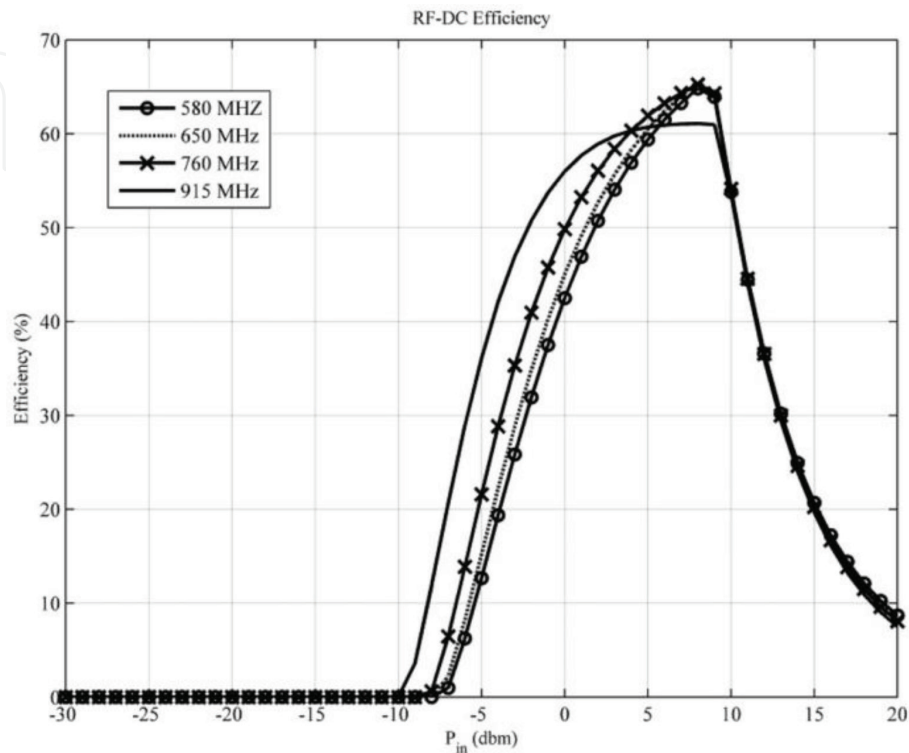


Figure 8.
Rectifier circuit efficiency.

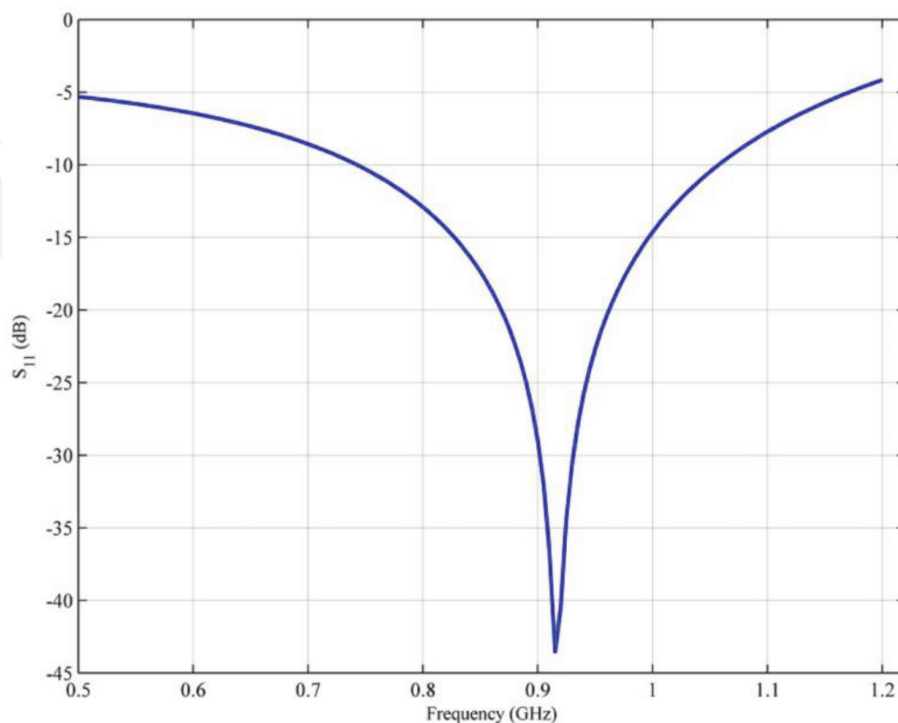


Figure 9.
Rectifier circuit return loss (s_{11}) at 0 dbm input RF power.

Figure 9 indicates the return loss (s_{11}) for different frequencies and minimum return loss is obtained at 915 MHz frequency at a circuit input power of 0 dbm. This is resulted from our designed matching circuit and shows its desirable performance.

In **Figure 10**, rectifier circuit output voltage and current are indicated with the maximum at 915 MHz.

For frequencies of 580, 650, 760 and 915 MHz, the outputs of voltage multiplier circuit are shown in **Figure 11**. As it can be seen, we obtain a 8.8 V DC voltage for our input signal.

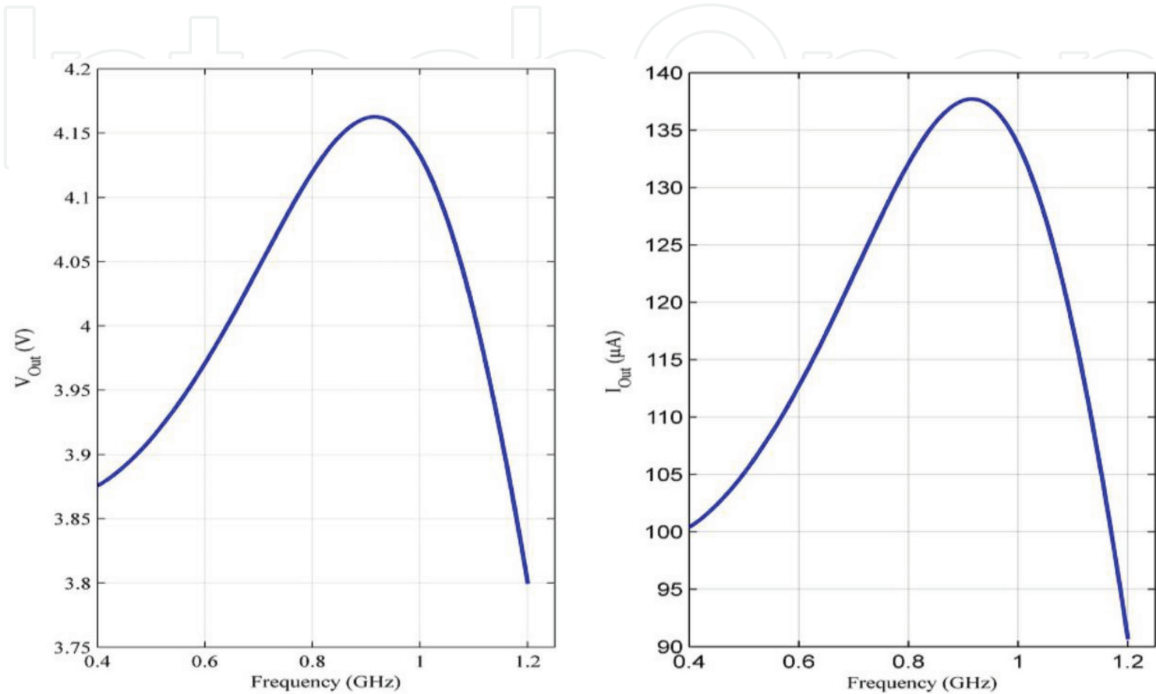


Figure 10.
Rectifier circuit output voltage and current.

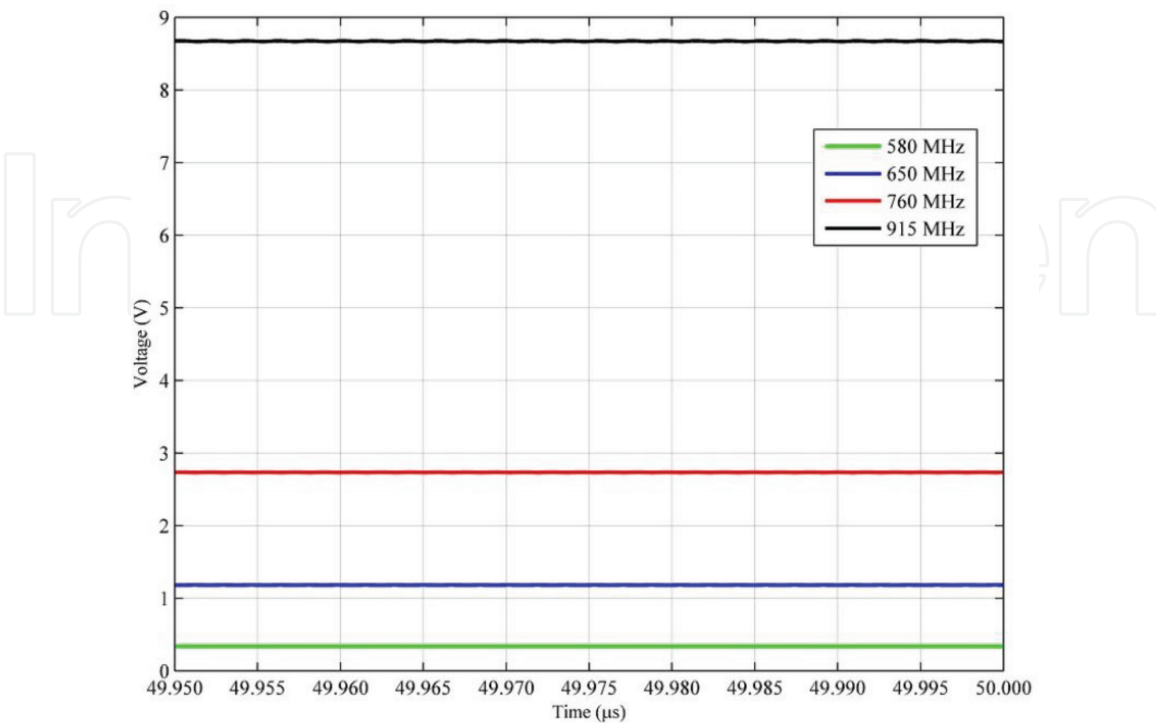


Figure 11.
Voltage multiplier circuit output.

Figure 12 shows the higher efficiency of our proposed circuit comparing to three other methods. That is because of exploiting a 10-stage voltage multiplier (a 4-stage connected to a 6-stage).

Complete charger circuit is proposed in **Figure 13**. Output currents for aforementioned four frequencies are given in **Figure 14**. Also, output voltages are

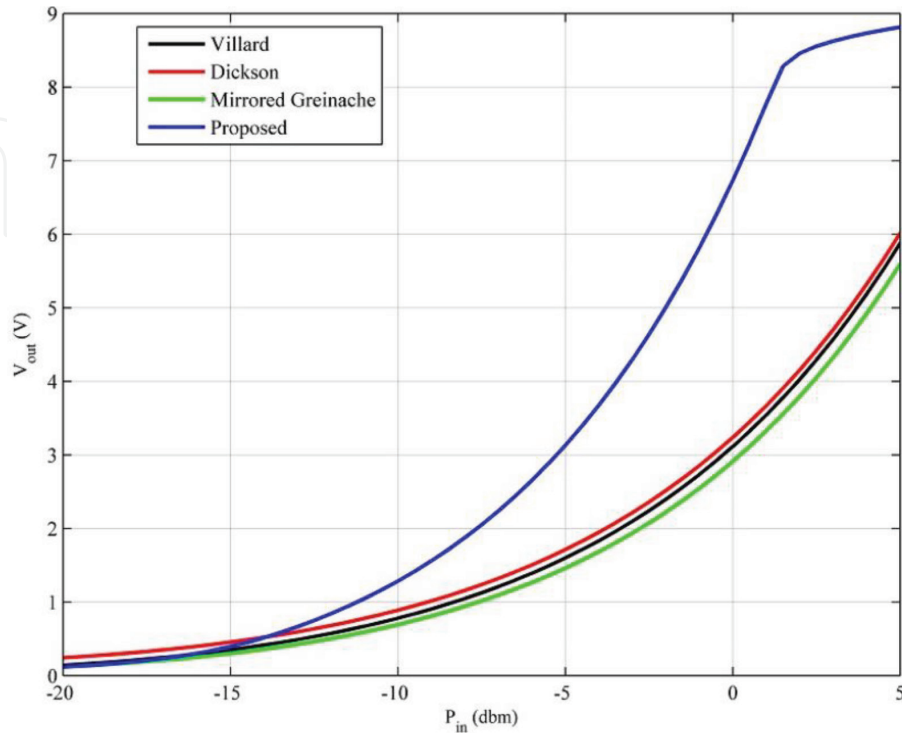


Figure 12.
 Output voltage versus input power.

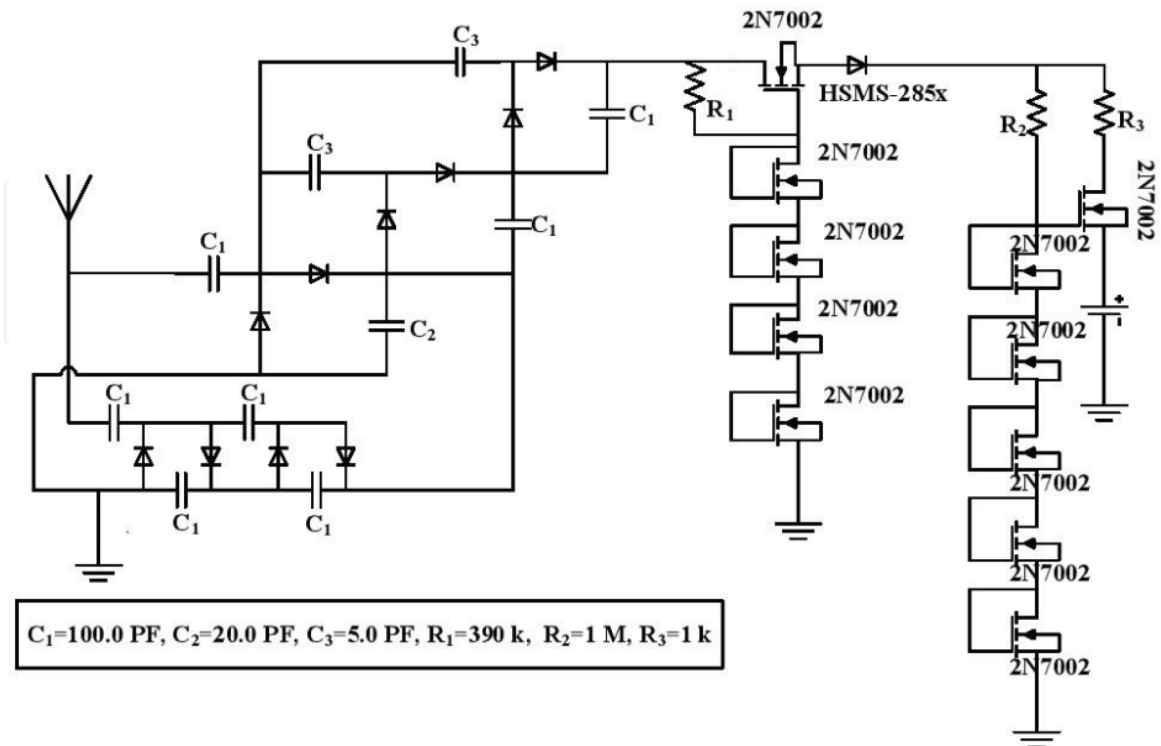


Figure 13.
 Charger circuit.

indicated in **Figure 15**. So knowing that power equals to current times voltage, we obtain $532\mu W$ output power for 915 MHz signal. It should be noted that voltage drop in 915 MHz (8.8 V to 3.6 V) is because that by connecting battery to charger circuit, battery charging process starts and in this process power must be constant, so by increasing the current drawn by the battery, output voltage drops.

3.3 Antenna simulation

Receiver antenna is a broadband type with linearly polarized radiation. Considering that our bandwidth is 500 MHz, according to previous experiences, we

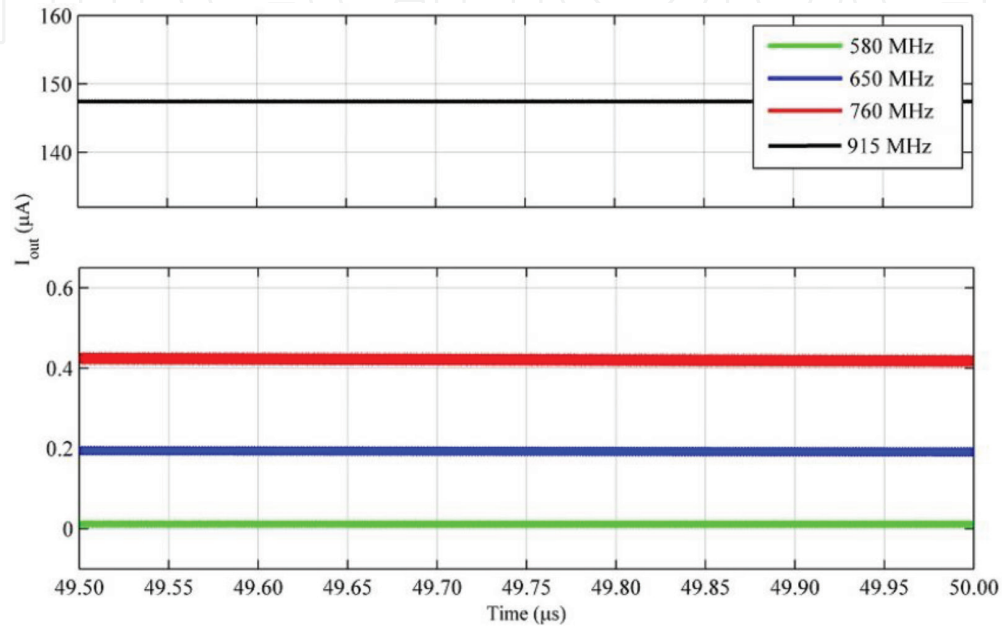


Figure 14.
Output currents in 580, 650, 760 and 915 MHz.

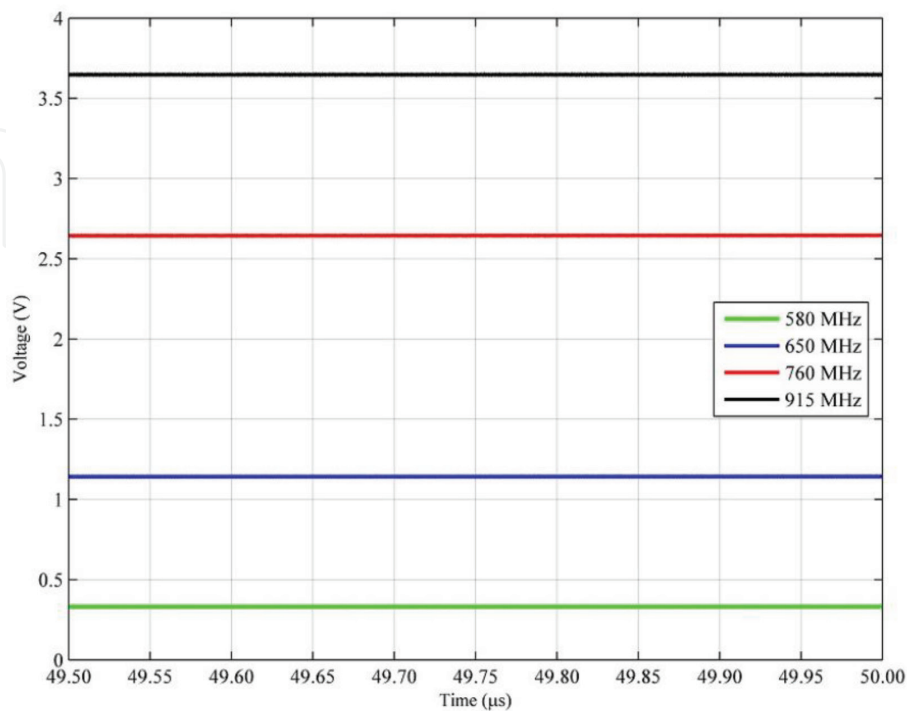


Figure 15.
Output voltages in 580, 650, 760 and 915 MHz.

require an Ultra Wide Band (UWB) antenna (**Figure 16**). By means of simulation and measurement, reflection coefficients of our designed antenna are indicated in **Figure 17**. Note that because of the size of this antenna, we did not use it obtain fabrication results. A challenge may be rise to decrease the size of UWB antenna and improve our designed system performance in the future.

3.4 Charger circuit fabrication

Test results for our fabricated charger circuit are indicated in **Figure 18**. In terms of experimental results, we obtain 6.89 V of output voltage at the frequency of 915 MHz (which obtained 8.8 V in simulation results), where our input signal is a 0 dbm generated by R&S®SMB100A signal generator. For a 10 k Ω resistive load, load voltage is 2.12 V and we can calculate the output power as 450 μ W.

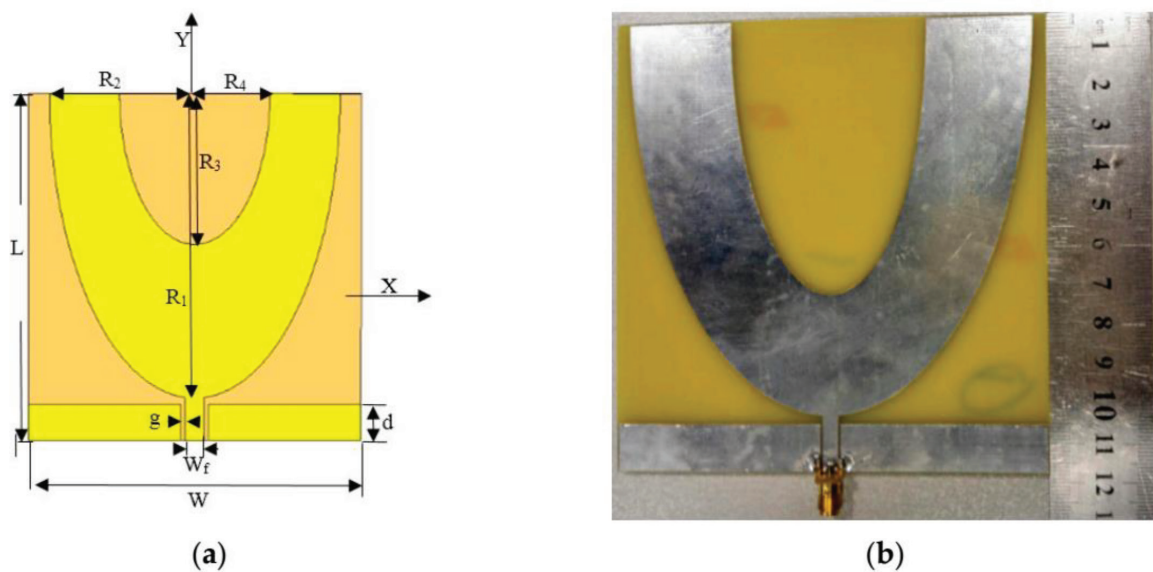


Figure 16.
Designed U-shape UWB antenna.

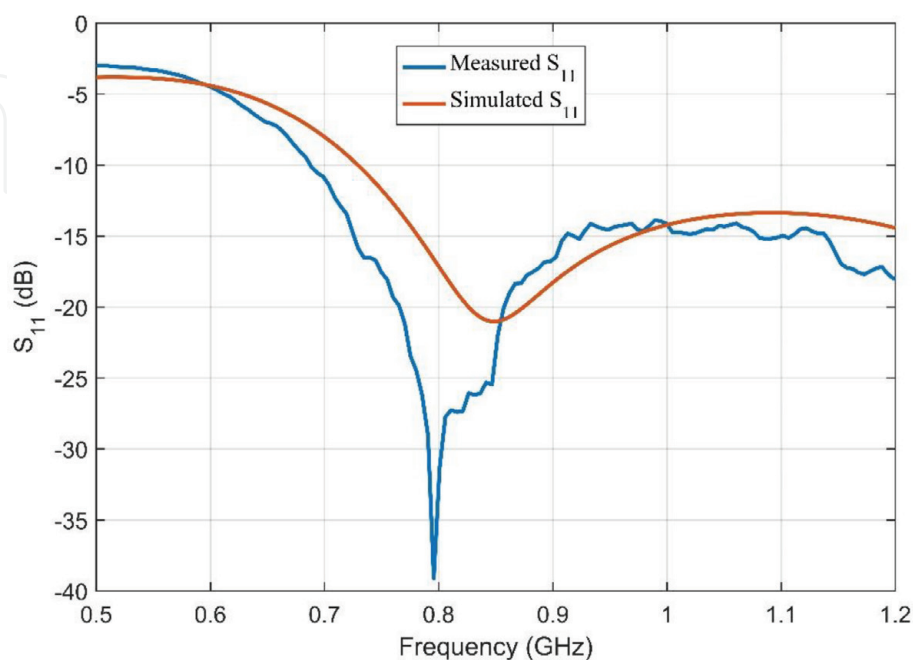


Figure 17.
Measured and simulated reflection coefficients of UWB antenna.

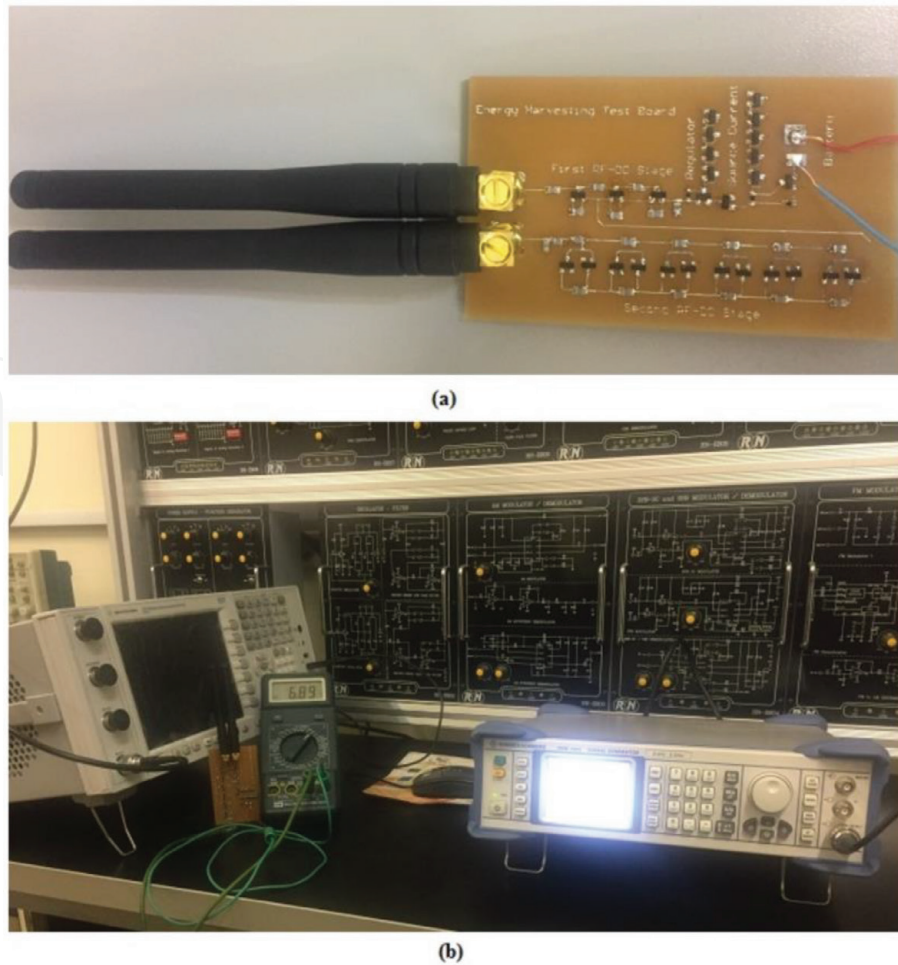


Figure 18.
(a) Fabricated charger circuit (b) Circuit test.

4. Conclusion

A novel approach for RF energy harvesting is presented in this chapter. Unlike previous works, we exploit spectrum sensing as a pre-processing procedure to find the frequency in which the maximum power more than a predefined threshold exists. After that, using a filter, this signal with maximum power is fed to a charger circuit. In simulation, a DC output voltage of 8.8 V is obtained using input RF power of 0 dbm. In practice and as our experimental results, our fabricated charger circuit test led to 450μ W output power for battery charging.

IntechOpen

IntechOpen

Author details


Naser Ahmadi Moghaddam^{1*} and Alireza Maleki²

1 Tarbiat Modares University, Tehran, Iran

2 K.N. Toosi University of Technology, Tehran, Iran

*Address all correspondence to: n.moghaddam1990@gmail.com

IntechOpen

© 2019 The Author(s). Licensee IntechOpen. This chapter is distributed under the terms of the Creative Commons Attribution License (<http://creativecommons.org/licenses/by/3.0>), which permits unrestricted use, distribution, and reproduction in any medium, provided the original work is properly cited. 

References

- [1] Soyata T, Copeland L, Heinzelman W. RF energy harvesting for embedded systems: A survey of tradeoffs and methodology. *IEEE Circuits and Systems Magazine*. 2016;**16**(1):22-57
- [2] Zhang JY, Cao Z, Wang Q, Kuwano H. Microstructure and piezoelectric properties of AlN thin films grown on stainless steel for the application of vibration energy harvesting. *IET Micro & Nano Letters*. 2012;**7**(12):1170-1172
- [3] Lafarge B, Curea O, Hacala A, Camblong H. Analysis, design & simulation of an electromechanical energy harvesting system using a linear movement. In: *International Conference on Green Energy*; 25-27 March 2014
- [4] Ali QI. Event driven duty cycling: An efficient power management scheme for a solar-energy harvested road side unit. *IET Electrical Systems in Transportation*. 2016;**6**(3):222-235
- [5] Azevedo JAR, Santos FES. Energy harvesting from wind and water for autonomous wireless sensor nodes. *IET Circuits, Devices and Systems*. 2012;**6**(6):413-420
- [6] Tan YK. *Sustainable Energy Harvesting Technologies—Past, Present and Future*. Rijeka, Croatia: InTech; 2011. Ch. 10
- [7] Paradiso J, Starner T. Energy scavenging for mobile and wireless electronics. *IEEE Pervasive Computer*. 2005;**4**(1):18-27
- [8] Intel Corp. Intel ambient RF energy harvesting demonstration [Online]. Available from: <http://www.rfwirelessensors.com/2009/01/intel-ambientrf-energy-harvesting-demonstration/>
- [9] Honan G, Gekakis N, Hassanalieragh M, Nadeau A, Sharma G, Soyata T. Energy harvesting and buffering for cyber physical systems: A review. In: *Cyber Physical Systems—A Computational Perspective*, ch. 7. 2015. United States: CRC; pp. 191-217. ISBN. 978-1-4822-5975-9
- [10] Impinj Inc. SPEEDWAY IPJ-R1000 Reader/Interrogator [Online]. Available from: <http://www.impinj.com/>
- [11] Sahai A, Cabric D. Spectrum sensing: Fundamental limits and practical challenges. In: *IEEE International Symposium on New Frontiers in Dynamic Spectrum Access Networks*, Baltimore, November; 2005
- [12] Kay SM. *Fundamentals of Statistical Signal Processing: Detection Theory*. 2nd ed. NJ, USA: Prentice Hall, Upper Saddle Rive; 1998
- [13] Urkowitz H. Energy detection of unknown deterministic signals. *Proceedings of the IEEE*. 1967;**55**(4):523-531
- [14] Gao W, Daut DG, Chen HS. Signature based spectrum sensing algorithms for IEEE802.22 WRAN. In: *IEEE International Conference on Communications*, Glasgow; 24-28 June 2007; pp. 6487-6492
- [15] Gardner WA. Exploitation of spectral redundancy in cyclostationary signals. *IEEE Signal Processing Magazine*. 1991;**8**(2):14-36
- [16] Han N, Shon S, Chung JH, Kim JM. Spectral correlation based signal detection method for spectrum sensing in IEEE802.22 WRAN systems. In: *The 8th International Conference on Advanced Communication Technology*, Phoenix Park; Vol. 3. 2006. pp. 1765-1770

- [17] Zeng Y, Liang YC. Covariance based signal detections for cognitive radio. In: 2nd IEEE International Symposium on New Frontiers in Dynamic Spectrum Access Networks, Dublin; 17-20 April 2007; pp. 202-207
- [18] Zeng Y, Liang YC. Maximum-minimum eigenvalue detection for cognitive radio. In: 18th International Symposium on Personal, Indoor and Mobile Radio Communications, Athens; 3-7 September 2007; pp. 1-5
- [19] Wornell GW. Emerging applications of multirate signal processing and wavelets in digital communications. *Proceedings of the IEEE*. 1996;**84**(4):586-603
- [20] Song L, Evans JW. Electrochemical-thermal model of lithium polymer batteries. *Journal of the Electrochemical Society*. 2000;**147**:2086-2095
- [21] Gomadam PM, Weidner JW, Dougal RA, White RE. Mathematical modeling of lithium-ion and nickel battery systems. *Journal of Power Sources*. 2002;**110**(2):267-224
- [22] Newman J, Thomas KE, Hafezi H, Wheeler DR. Modeling of lithium-ion batteries. *Journal of Power Sources*. 2003;**119-121**:838-843
- [23] Pedram M, Wu Q. Design considerations for battery-powered electronics. In: *Proceedings of the 36th Annual ACM/IEEE Design Automation Conference*; 1999. pp. 861-866
- [24] Rynkiewicz R. Discharge and charge modeling of lead acid batteries. *Applied Power Electronics Conference and Exposition*. 1999;**2**:707-710
- [25] Rakhmatov D, Vrudhula S, Wallach DA. A model for battery lifetime analysis for organizing applications on a pocket computer. *IEEE Transactions on VLSI Systems*. 2003;**11**(6):1019-1030
- [26] Rong P, Pedram M. An analytical model for predicting the remaining battery capacity of lithium-ion batteries. *IEEE Transactions on Very Large Scale Integration (VLSI) Systems*. 2006;**14**(5):441-451
- [27] Valvo M, Wicks FE, Robertson D, Rudin S. Development and application of an improved equivalent circuit model of a lead acid battery. In: *Proceedings of the 31st Intersociety Energy Conversion Engineering Conference*. Vol. 2. 1996. pp. 1159-1163
- [28] Ceraolo M. New dynamical models of lead-acid batteries. *IEEE Transactions on Power Systems*. 2000;**15**(4):1184-1190
- [29] Barsali S, Ceraolo M. Dynamical models of lead-acid batteries: Implementation issues. *IEEE Transactions on Energy Conversion*. 2002;**17**(1):16-23
- [30] Gao L, Liu S, Dougal RA. Dynamic lithium-ion battery model for system simulation. *IEEE Transactions on Components and Packaging Technologies*. 2002;**25**(3):495-505
- [31] Glass MC. Battery electrochemical nonlinear/dynamic SPICE model. In: *Proceedings of the 31st Intersociety Energy Conversion Engineering Conference*. Vol. 1. 1996. pp. 292-297
- [32] Baudry P, Neri M, Gueguen M, Lonchamp G. Electro-thermal modeling of polymer lithium batteries for starting period and pulse power. *Journal of Power Sources*. 1995;**54**(2):393-396
- [33] Hageman SC. Simple pspice models let you simulate common battery types. *EDN*. 1993;**38**:17-132
- [34] Chen M, Rincon-Mora GA. Accurate electrical battery model capable

of predicting runtime and I-V performance. *IEEE Transactions on Energy Conversion*. 2006;21(2)

[35] Nyquist H. Abridgment of certain topics in telegraph transmission theory. *Journal of the A.I.I.E.* 1928;47(3):214-217

IntechOpen

IntechOpen